Initiation of electrical discharge at the triple junction of the lightning protection of an aircraft radome

F. Padoan, D. Clark, A. Haddad.

Morgan-Botti Lightning Laboratory,

Advanced High Voltage Engineering Research Centre, School of Engineering, Cardiff University, CF24 3AA

PadoanF@cardiff.ac.uk, Haddad@cardiff.ac.uk, ClarkD@cardiff.ac.uk.

C. Karch, P. Westphal

Cross Domain System Engineering – TEYYX

Airbus Defence and Space GmbH,

Rechliner Straße, 85077 Manching, Germany

christian.karch@airbus.com, peter.westphal@airbus.com

ABSTRACT

The shape of the radar antenna and its lightning protection diverter strips can cause air ionization and streamer inception, which may lead to lightning attachment. In this paper, we are particularly investigating the field enhancement at the triple junction point formed by the metallic diverter strip, the radome material and the surrounding air. In this work, a tangent ogive shape radome geometry has been implemented in the simulation, adopting the EUROCAE standard configuration for lightning laboratory tests, to compute the magnitude of electric fields in the dielectric material and its surrounding air, and to evaluate the temperature conditions at the triple junction point using Magnetohydrodynamic equations. Various solid diverter strip design geometries have been then considered with the aim to control the discharge initiation and reduce the electromagnetic shielding effect on the radar's electromagnetic signal.

Laboratory tests were conducted on a commercial aircraft radome to validate the simulations.

Keywords: aircraft radome; lightning protection, numerical simulations, Triple junction point, Lightning testing.

1. INTRODUCTION

Aircraft radomes are often subjected to corona effects and electrical arcing under lightning strike conditions. These affect aircraft radomes when extremely high electric fields are generated during flight in the proximity of charged cumulonimbus clouds. The radome dielectric material and antenna system is commonly protected against lightning using segmented or solid diverted strips. These devices have been widely used and tested ([4],[5],[6],[7]), in order to ensure at the same time safety and transparency to the radar's electromagnetic communication signals.

Numerical simulations can predict where the attachment point might occur in a high electric field. These preliminary evaluations highlighted a spike in the electrical field magnitude close to the triple junction point (TPJ) formed at meeting location of the strips, dielectric material of the radome, and the air [8]. When sufficiently high, this field may cause air ionization, streamer formation and/or undesirable onerous puncture of the radome wall following dielectric breakdown.

Using numerical field computations, it is possible to predict and optimise the point where the discharge might occur, while considering the antenna pattern at the same time. In this work, numerical field simulations were performed using COMSOL Multiphysics to study a laboratory high voltage test configuration, in which various voltage shapes are applied to a high voltage electrode pointing in the direction of a test radome equipped with solid diverter strips. Different spatial diverter strip configurations were studied to clarify the shielding effect and, where possible, determine the location points of lightning attachment.

A further study has been undertaken to model effects due to high temperature and pressure using magnetohydrodynamics equations when the lightning arc is already established. Very high temperatures have been found in proximity to the attachment point, which might lead to a thermally induced dielectric breakdown and changes in the electrical properties of the radome material. To validate the numerical results, laboratory tests were undertaken in the High Voltage Laboratory at Cardiff University. A radome of a commercial aircraft has been studied under a high electric field generated by a sphere electrode energized with a high voltage DC generator. This allows comparison of measured and simulated locations of discharge initiation as well as the magnitude of applied voltage.

2. ANALYTICAL, NUMERICAL AND PRACTICAL APPROACHES IN PREVIOUS WORKS

As it is not possible to perform controlled practical tests on lightning strikes on aircraft in flight, risking the safety of the plane and the crew inside it, a series of models and laboratory tests have been developed, according to existing current standards, as described in EUROCAE ED-105A [9]. The circuit in Fig.1 is proposed [9] to validate the radome lightning protection system.

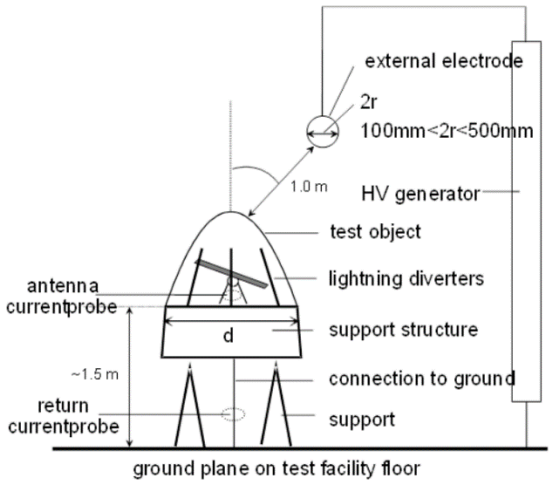

Figure 1: Adapted laboratory radome test setup according to EUROCAE ED-105A. [9]

Different approaches have been considered by previous researchers to ensure a suitable solution for the aircraft safety and performance. In [10], an analytical solution shows how the electrical field inside the radome reaches very high magnitude. Considering a simplified geometry and an applied constant electric field, it was found that the magnitude of the

critical ambient field is $E_{cr} \approx 50\ to\ 80\ kV/m$ is necessary to launch leaders from the aircraft tip, which agrees with the fields measured inside a storm-cloud. In [7], an electrostatic model was implemented to evaluate the electrical field effect at the diverter strip on a sample of dielectric material, and the influence on the antenna gain changing with different strip positions has also been studied. In contrast, in [5], a radome geometry has been developed in a laboratory configuration: different diverter strip geometries with and without the radome were simulated, evidencing the charge distribution on the surface of the radome considering different voltage waveforms. In [11], using a Magnetohydrodynamic model, the current and best design of segmented diverter strips were predicted in order to obtain the best discharge conditions once the positive and negative leaders have connected, and the return stroke is initiated. In [12], the geometry and structure of segmented diverter strips are described together with their behaviour under lightning strike. Both laboratory tests with and without diverter strips were considered to describe the breakdown conditions. Some interesting results were obtained proving that: "The segmented strip may be viewed as a series of conductors, each with a stray capacitance to the air frame" [12]. Other important works regarding long sparks discharges and interaction of radome with aircraft have been completed, contributing to clarification of the physics of the discharge as reported in [13] [14] [15] and to the charge accumulation in a cumulonimbus cloud as described in [16].

In this paper, the finite element method has been implemented to highlight different aspects of the discharge on the diverted strips. First, Maxwell equations were solved to study the attachment point. Then, possible damages to the structure due to high temperatures and pressures caused by lightnings strikes were considered.

3. NUMERICAL SIMULATIONS

3.1 Attachment point evaluation

A first step of the numerical simulation process has been an electromagnetic simulation on the radome structure, as used in a laboratory test arrangement, similar to the setup shown in Fig. 2. For the simulation studies, the test voltage waveforms A and D with both polarities have been adopted and assigned to the high voltage external electrode to determine the electric field distribution in each case.

3.2 Geometry

In order to obtain an accurate simulation of the electric field, the radome geometry was built in SolidWorks, using realistic aircraft's nose radome dimensions. The inner height of the tangent ogive radome is $L_{in} = 1.504$ m and the inner base radius is $R_{in} = 0.475\ m$. The inner ogive radius is $\rho_{in} = 2.6186\ m$.

Following this dimensioning, a monolithic radome was built with a thickness of 10.013 mm. Then, the support was built, considering at first a parabolic antenna with the following dimensions: D -d/D =0.05, where D is antenna diameter, d is antenna height. D has been chosen 0.5 m and d=0.05 m. The base has a diameter of 0.97 m and a height of 0.20 m. Finally, the strips need to be built on the external surface of the radome, which was achieved with an extruded cut of 5 mm on the radome surface. Strips with a height of 0.80 m and a width of 0.02 m were considered. using the CAD import tool in COMSOL Multiphysics, the geometry described above was imported for further processing in COMSOL, as shown in Fig. 2. The radome structure is placed inside a spherical domain of r=3m, to which is also introduced a spherical high-voltage electrode of r=0.1m, as illustrated in Fig.3.

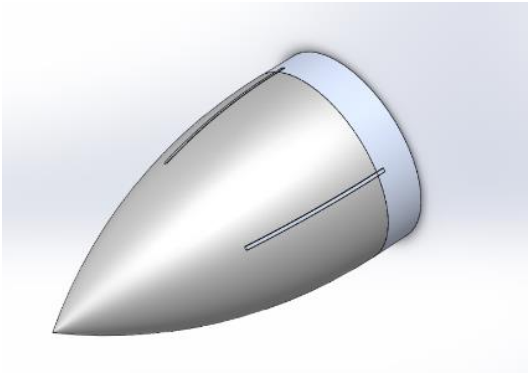

Figure 2:Radome geometry, solid strips, radar and base.

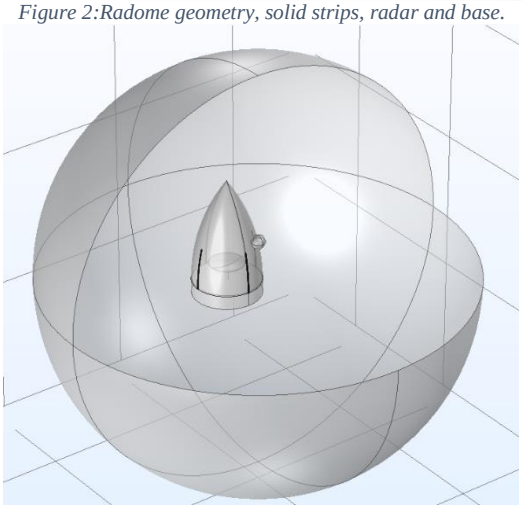

Figure 3: Radome geometry imported in COMSOL M*ultiphysics. The external spherical domain, and the electrode have been built in the FEM software.*

3.3 Materials

The radome was set as a glass fibre material having a relative permittivity $\varepsilon_r = 3.3$ and a very low conductivity of $0.0001\ S/m$. Antistatic paint will be set in the Physics section described below as a Boundary condition in order to avoid problems with the meshing process of the geometry. The base of the radome, the antenna and the strips are modelled as copper. The choice of the conductor is not very important at this stage, since high currents are not considered here, but the high conductivity ensures redistribution of charges in the copper. The remaining domains were set as Air.

3.4 Physics and Boundary Conditions

For this problem, an electric current simulation has been chosen.

- a voltage waveform A of peak voltage $1\ MV$ applied to the electrode using a double exponential shape, defined as:

$$V = 1050 \cdot \left(e^{-\frac{t}{70[\mu s]}} - e^{-\frac{t}{0.40[\mu s]}} \right) [kV] \quad (1)$$

- afterwards, a voltage waveform D, having peak value of $1\ MV$ applied to the electrode in order to evaluate how charges distribute when considering a longer impulse time:

$$V = 1050 \cdot \left(e^{-\frac{t}{2000[\mu s]}} - e^{-\frac{t}{20[\mu s]}} \right) [kV] \quad (2)$$

- A ground condition ($V = 0\,V$) at the base, strips and antenna surface.
- an "electric shielding" boundary condition is imposed on the outer radome surface:

$$n \cdot (J_1 - J_2) = -\nabla \cdot d_s(\sigma \nabla V) \qquad (3)$$

Where d_s is the layer thickness, J_1 and J_2 are the current densities in air and antistatic paint, respectively.

3.5 Mesh

To achieve a good resolution while solving the discussed problem, a user-defined mesh has been built with a final 945,259 domain elements, 156,879 boundary elements and 10,738 edge elements.

3.6 Simulation Results

At first, the effect of the two voltage waveforms on the radome surface has been studied, considering the system just with the base and antenna, then with the radome and strips and finally considering also the antistatic paint. As can be seen in Fig.4, the results indicate that, using the voltage waveform A, the shielding effect provided by the strips and the antistatic paint decreases the charge accumulation on the antenna, resulting in a lower electric field. Similar results were achieved in [5].

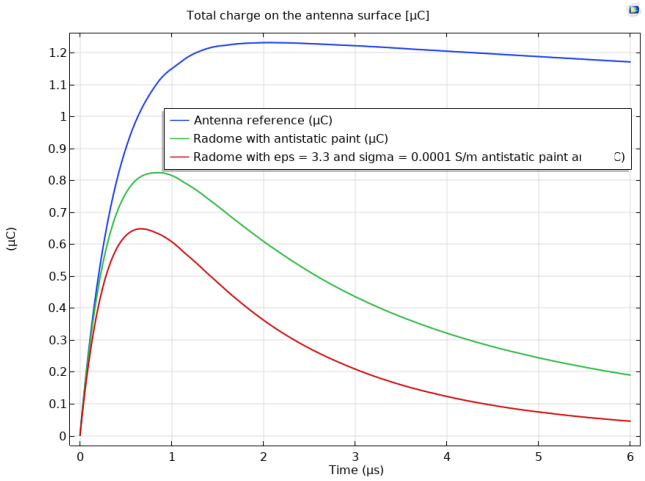

Figure 4: Total charge accumulation on antenna surface, considering, imposing Voltage Wave A. The system without radome (Antenna reference, blue line) follows the voltage waveform. Considering the radome and then also the antistatic paint (Green and red line) the electric field is highly reduced due to the different charge distribution.

Using the voltage waveform D, the benefit of the strips and antistatic paint is more effective, even if the paint conductivity has a low value. This is clearly illustrated in Fig. 5.

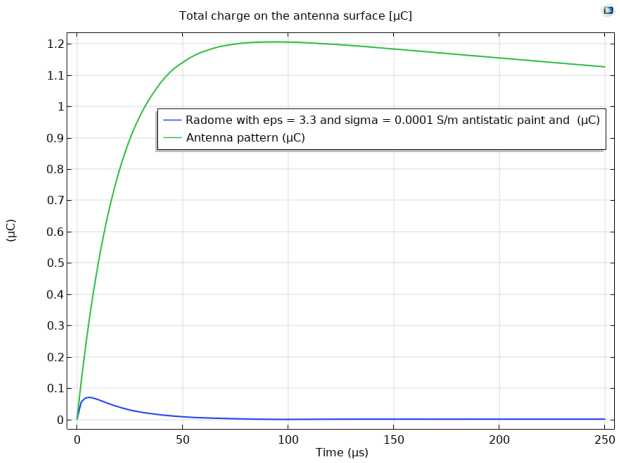

Figure 5: Total charge accumulation on antenna surface, considering, imposing Voltage Wave B.

The above results highlight the importance of considering the electric field distribution and the effect of conductivity and dielectric losses to account for charge movement and ensure conduction electrical currents are in phase with the electrical field.

The most interesting feature in this simulation is the electric field magnitude spike close to the triple junction point, as indicated in Figs. 6 and 7. Here, the radome material dielectric strength could be exceeded, causing the so-called "radome puncture" due to intrinsic electric breakdown.

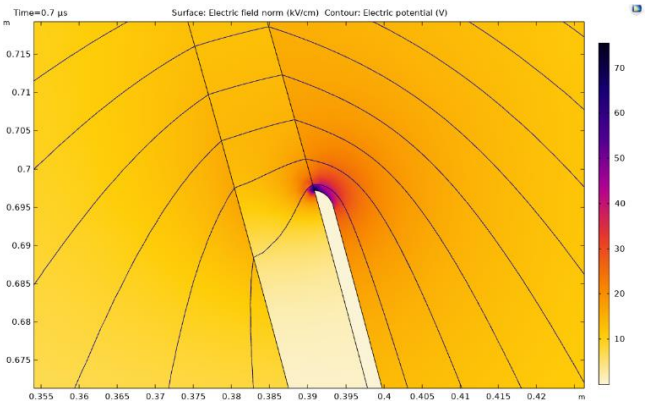

Figure 6: 2D equipotential lines on a detail at the diverter strip tip. The electric field at the triple junction point reaches values high enough which may cause the dielectric breakdown of the radome.

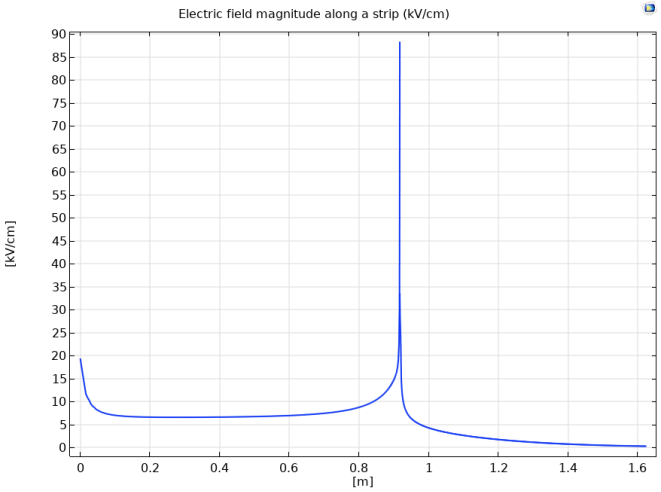

Figure 7: Electric field magnitude along a diverter strip

In order to assess this problem of high electric field, different strip geometries have been studied in this work:

- Using double diverter strips, one outside and one inside, in order to create a fictious smoother edge at the tip of the strips,
- Using internal diverter strips, linked to the surface using apposite screws,

The two options might create a situation of dielectric overheating having extremely high currents flowing through them, and the possibility of a discharge between the strip and the antenna.

3.7 MHD approach to evaluate hotspots at the triple junction point

An important aspect to take into account is to evaluate at first if, at the attachment point, the electric field conditions are high enough to cause a damage due to extreme temperatures and pressures in that small area. To study the effects of the current flowing through the conductor, it is possible to assume that

positive and negative leaders have already connected with each other, and the breakdown has occurred. For this reason, a thermal plasma can be considered, in which, having a pressure of 1 atm and a high temperature ($T > 10\,000\,°C$), it is possible to consider that there are so many collisions that the electrons and heavy particles have the same average speed. This is a fundamental assumption because we can consider plasma like a "conductive fluid", and hence use the Magnetohydrodynamic equations.

$$\frac{\partial \rho}{\partial t} + \nabla \cdot \rho V = 0 \quad (4)$$

$$\frac{d\rho V}{dt} = -\nabla p - \frac{1}{c} J \times B \quad (5)$$

$$E + \frac{V \times B}{c} = \eta J \quad (6)$$

$$\nabla \cdot E = \frac{\rho_c}{\varepsilon_0} \quad (7)$$

$$\nabla \cdot B = 0 \quad (8)$$

$$\nabla \wedge E = -\frac{\partial B}{\partial t} \quad (9)$$

$$\nabla \wedge B = \frac{j_s}{\varepsilon_0 c^2} + \frac{1}{c^2}\frac{\partial E}{\partial t} \quad (10)$$

Where ρ is the mass density $[kg/m^3]$, V is the local mean velocity of particles $[m/s]$, J is the current density $[A/m^2]$, ρ_c is the charge density $[C/m^3]$, B is the induced magnetic field [T], E is the electric field [V/m], ε_o is the dielectric constant in vacuum.

Other assumptions that are needed for an MHD model are: the arc is considered stationary, an axisymmetric coordinate system is used, the plasma is a single weakly compressible Newtonian fluid and is assumed to be argon at Local Thermodynamic Equilibrium (LTE), the convection generated by the Lorentz forces can be treated as a laminar flow, and the gravity effects can be neglected. Throughout, atmospheric pressure is assumed.

Previous simulation work [17-24] describes the temperature and pressure conditions on the fuselage of an aircraft. These used a discharge between an electrode and a copper plate, with a gap from 3 mm to 50 mm.

3.8 Geometry

A simple geometry, as shown in Fig. 8, has been considered which is similar to that in [17]. It has a tungsten cathode and a plain aluminum anode with a gap of 10 mm filled with argon.

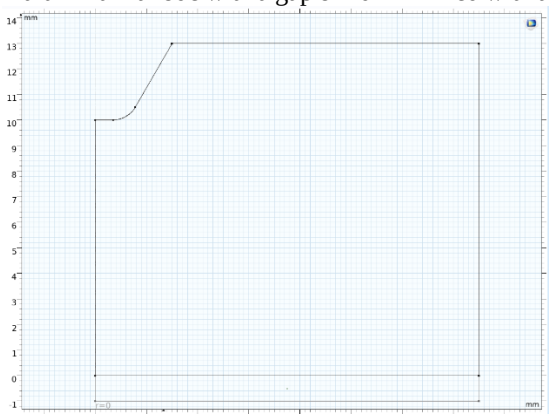

Figure 8:Axialsymmetric Geometry built in COMSOL Multiphysics.

3.9 Physics and Boundary conditions

In COMSOL coupling of the electric current, magnetic field, laminar flow and heat transfer is possible.

For Electric Current: A linear discretization has been chosen in order to have a faster solution. A ground condition is taken at the base of the anode, and a normal current density condition is considered at the tip of the cathode. The current is assumed to decrease exponentially in the radial direction, r, according $to\ J_z(r) = J_{max} e^{-br}$. With $b = 1364.54 m^{-1}$, we have $J_{max} = 1.2 \cdot 10^8 A \cdot mm^{-2}$. A current magnitude I = 200A is adopted.

$$I = 2\pi \int_0^{R_c} J(r) dr \quad (11)$$

with R_c the cathode radius.

For Magnetic field: An 'in-plane' condition has been imposed on the basis that the magnetic field will be perpendicular to the 2D plane.

For Heat transfer in solid and liquids: A 300 K temperature has been imposed in the argon domain with 1,000 K at its boundary. The Boundary heat source set to the electrodes in order to have the radiation cooling from the solid to the gas. An initial temperature of the plasma column of 10,000K has been imposed.

For Laminar flow: In order to avoid a too high computational cost, a weakly compressible flow condition is enough to achieve good results. An open boundary condition has been applied.

3.10 Results

The arc formed in the simulation depicts a situation in which very high gas temperatures are created between the cathode and the conductive plate. In a radome situation, this might be a problem since, even if the attachment point is on the strips, the temperature on the surrounding dielectric could be high enough to change the material characteristics with a subsequent breakdown and puncture of the structure.

As indicated in Fig.9, the maximum temperature in this model is 23700 K, which close to the result obtained in [17], with a value of 21 700 K. Further studies will be needed in future studies to properly evaluate the interaction between the gas and the conductor and considering the dielectric.

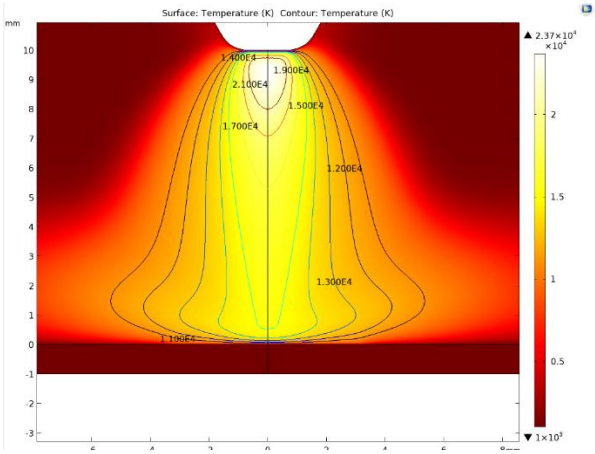

Figure 9: Temperature profile between the cathode and the aluminum plate, evidencing a maximum temperature of $2.37 \cdot 10^4$ *[K].*

4. LABORATORY MEASUREMENTS

To determine and verify the model for the inception location in a radome structure, a laboratory test was performed on a Boeing-737 aircraft radome.

A condition of high electric field has been created on the radome surface, and Ultraviolet (UV) cameras have been used to detect partial electrical discharges at the diverter strips.

4.1 Laboratory setup

In order to reach that condition, the circuit depicted in Fig.10 was adopted applying the high voltage energisation to a spherical electrode close to the radome. Both the applied

voltage and the current flowing through the strips were measured.

The circuit consists of a DC HV (Direct Current High Voltage) generator, a voltage divider and the electrode/radome test object. The HV Generator is an LH Open Stack Series capable of delivering a maximum value of 100 kV positive direct voltage. The spherical electrode, as seen in Fig. 11, has a diameter of 25 cm and can be moved both horizontally and vertically. The diverter strips conductors were all bonded together and grounded except the one closest to the spherical electrode. The radar antenna was simulated with a grounded circular plate of 1 m diameter.

The currents through the various grounding points of the test object were measured with shunt resistors. A UV Camera: Camera was used to detect the presence of partial/corona discharges on the test radome.

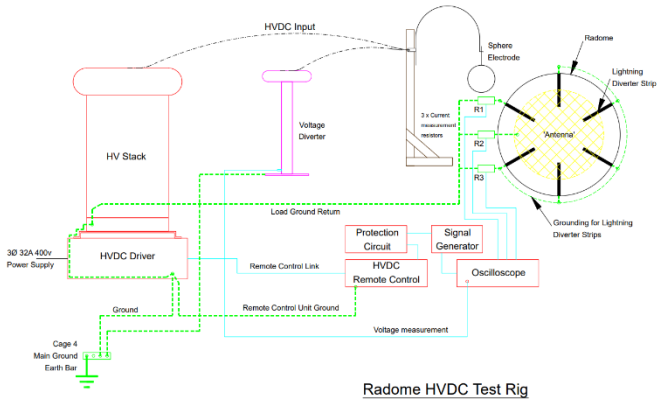

Figure 10: Laboratory setup to evaluate the inception point on a Boeing-747 Radome.

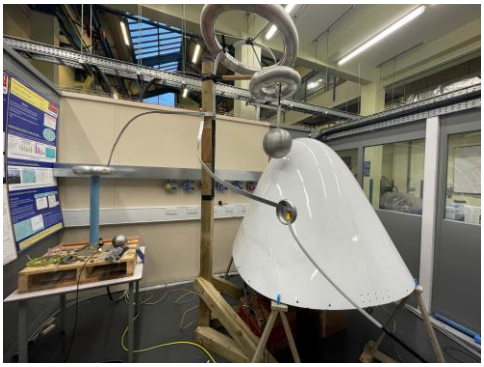

Figure 11: Laboratory setup.

Before starting the tests, a COMSOL simulation has been run to predict the electric field distribution and magnitude (Fig.12) which allowed to estimate the spacing required between the spherical electrode and diverter to reach discharge inception.

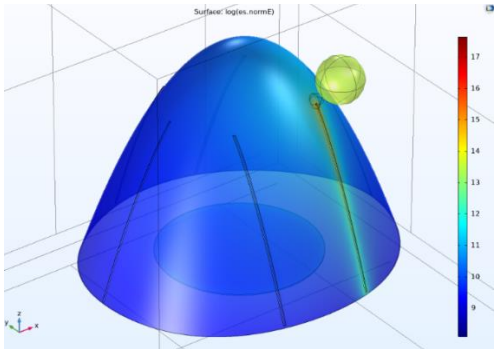

Figure 12: Electric field on the radome, applying a 100 kV voltage on a spherical electrode.

4.2 Test procedure and results

Different tests have been conducted on the radome structure, changing the positions of the electrode and radome. At first, no activity has been captured from the system. This was attributed to the presence of antistatic paint applied on the structure. In order to avoid this problem, paint was removed from a small area near the tip of the diverter strip. With this modification and for a 10 cm electrode gap, electrical discharge activity was detected, as shown in Fig. 13. As can be seen on the figure, a peak current value of 5 mA was measured with 80 kV applied voltage.

Fig.14 clearly demonstrate the impact of the electrical discharge on the diverter strip conductor. The conductor tip, where the triple junction point is located, is clearly subjected to severe electrical discharge erosion when a higher value of 100 kV was applied for a short period, which caused a flashover, hence the extensive erosion of the strip. It is worth highlighting that lightning strike current magnitude is much higher than that of the flashover current due to the limited power of the DC supply, and hence it is is expected to cause a more severe erosion at the attachment point.

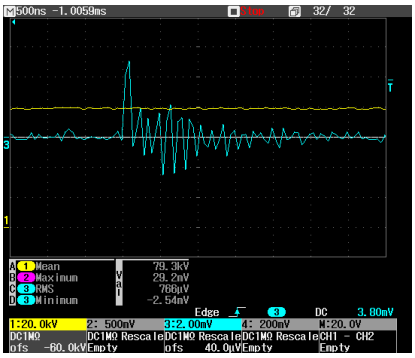

Figure 13: example of Partial discharge activity signal seen on the oscilloscope.

Figure 14: Boeing 737 diverted strip tip. the yellow material is the dielectric material underneath the antistatic paint and the black parts show the metal erosion at the attachments points of flashover event.

4.3 Comparison with numerical results

The aim of the test experiment was to verify the initiation point of a streamer/leader formation on a radome in a high electric field condition. As shown in Fig. 14, the breakdown occurred on the system exactly on the points where the peak of the electric field was expected from the numerical simulations (Fig.7).

The low current value of the discharge didn't damage the radome structure deeply, but in case of a lightning strike the temperature and pressure conditions might be extreme for the dielectric material in close contact with the strips, as show in section 3.2. The radome degradation might bring to a change in its conductivity, and the discharge could cause a puncture, dangerous for the navigation system and for the aerodynamic characteristic. Further evaluations will be done in the

Advanced High Voltage Engineering Research to find a solution that might decrease the electric field peak value of the electric field from the TJP to other conductive parts of the diverted strip.

5. CONCLUSIONS

In this paper, the radome lightning protection diverter strips were analysed to study electrical discharge initiation from an aircraft radome.

Different numerical simulations have been used to evaluate where the attachment point of a long spark might occur. It has been highlighted that the triple junction point is a region where the electric field may reach magnitudes high enough to cause dielectric breakdown with possible consequent puncture of the dielectric radome wall structure which, in turn, may cause aerodynamic problems and damage to the radome material.

Experimental high voltage tests were carried out to generate an electric field magnitude high enough to cause an initial partial discharge from the tip of diverter strips mounted on a real commercial aircraft radome.

It was shown that removal of the antistatic paint allows better observation of electrical discharge activity at the triple junction point. Under high applied external electric fields, flashover occurs causing significant erosion of the conductor at triple junction location.

6. ACKNOWLEDGEMENTS

The authors would like to thank Endeavr and AIRBUS Defense and Space Manching for the financial support.

7. REFERENCES

[1] D. Morgan, C.J. Hardwick, S.J. Haigh, A.J. Meakins. “The Interaction of Lightning with Aircraft and the Challenges of Lightning Testing”. AerospaceLab, p. 1-10, 2012. ffhal-01184419f

[2] Eurocae ED-14E: “ENVIRONMENTAL CONDITIONS AND TEST PROCEDURES FOR AIRBORNE EQUIPMENT – Lightning direct effects”, July 2013

[3] EUROCAE ED-84, “Aircraft Lightning Environment and Related Test Waveforms Standards”, July 2013.

[4] C. Karch, C. Paul, F. Heidler, “Lightning strike protection of radomes”, 2019 International Symposium on Electromagnetic Compatibility - EMC EUROPE, 17 October 2019, 10.1109/EMCEurope.2019.8871944.

[5] C. Karch, W. Wulbrand, and H.W. Zaglauer, “An approach to determining radome diverter strip geometry”,Blackpool, UK, International Conference on Lightning and Electricity (ICOLSE), Volume 2, 2003.

[6] C. Karch , W. Lick , and S. Pack, “FULL-SCALE HIGH VOLTAGE RADOME INITIAL LEADER ATTACHMENT TESTS”, 2019 International Conference on Lightning and Static Electricity, Wichita, US,2019.

[7] D. Yanchao, X. Xiu and H. U. Pingdao, "Research on aircraft radome lightning protection based on segmented diverter strips," 2017 International Symposium on Electromagnetic Compatibility - EMC EUROPE, 2017, pp. 1-6, doi: 10.1109/EMCEurope.2017.8094806.

[8] M, Banda, D, Malec, J-P. Cambronne, “Simulation of Space Charge Impact on Partial Discharge Inception Voltage in Power Busbars Dedicated to Future Hybrid Aircrafts. Circuits and Systems”, 2018, 09 (11), pp.196-212. ff10.4236/cs.2018.911018ff. ffhal-02182458

[9] Eurocae ed-105a: “Aircraft lightning test methods.”, July 2013.

[10] N.I. Petrov, A. Haddad, H. Griffiths, R.T. Waters, “Lightning strikes to aircraft radome: electric field shielding simulation proc.”, 17th Int. Conf. on Gas Discharges and their Applications, 513-516 (Cardiff, UK), September 8 - 11 2008.

[11] H. Chen, Fusheng Wang, Xiu Xiong, Zheng He, Zhufeng Yue, “Plasma discharge characteristics of diverter strips subject to lightning strike”, Plasma Sci. Technol., Volume 21, No. 2, 28 November 2018.

[12] J.A Plumer, L.C. Hoots, “Lightning protection with segmented diverters”, IEEE Int. Symp. On Electromagnetic Compatibility, Atlanta, Georgia, USA, 1978. https://doi.org/10.1109/isemc.1978.7566854

[13] I. Gallimberti. “The mechanism of the long spark formation.” Journal de Physique colloques, 40 (c7), pp.c7-193-c7-250, 1979. Ff10.1051/jphyscol:19797440ff. Ffjpa-00219444

[14] A. Bondiou and I. Gallimberti, “Theoretical modelling of the development of the positive spark in long gaps” J. Phys. D: Appl. Phys., Vol.27, pp.1252-1266, 1994.

[15] N. Goelian, P. Lalande, A. Bondiou-Clergerie, G.L. Bacchiega, A. Gazzani, I. Gallimberti, “A simplified model for the simulation of positive-spark development in long air gap”, J. Phys. D: App. Phys. Vol.30, pp.2441-2452, 1997.

[16] P. Lalande, V. Mazur, “A physical model of branching in upward leaders”, AerospaceLab Journal, AL05-07, December 2012.

[17] F Lago, J. J. Gonzalez, P. Freton and A. Gleizes, “A numerical modelling of an electric arc and its interaction with the anode: Part I. The two-dimensional model”, Journal of Applied Physics vol. 37 Number 6, 24 February 2004.

[18] J J Gonzalez, F Lago, P Freton, M Masquere and X Franceries, “Numerical modelling of an electric arc and its interaction with the anode: part II. The three-dimensional model—influence of external forces on the arc column”, Journal of Applied Physics vol. 38 Number 2, 6 January 2005. https://doi.org/10.1088/0022-3727/38/2/016.

[19] F. Wang , X. Ma, H. Chen and Y. Zhang, “Evolution simulation of lightning discharge based on a magnetohydrodynamics method”, Plasma Science and Technology, Vol 20, Number 7, 23 May 2018, https://doi.org/10.1088/2058-6272/aab841

[20] M. Khalil, N. Abuelfoutouh, G. Abdelal, A. Murphy, “Numerical Simulation of Lightning Strike Direct Effects on Aircraft Skin Composite Laminate”, International Journal of Architectural and Environmental Engineering Vol:12, No:2, 2018.

[21] G. Abdelal and A. Murphy, “A Multiphysics Simulation Approach for Efficient Modeling of Lightning Strike Tests on Aircraft Structures”, IEEE TRANSACTIONS ON PLASMA SCIENCE, VOL. 45, NO. 4, APRIL 2017.

[22] F Lago, J J Gonzalez, P Freton, F Uhlig, N Lucius and G P Piau, “A numerical modelling of an electric arc and its interaction with the anode: part III. Application to the interaction of a lightning strike and an aircraft in flight”, Journal of Applied Physics, Vol.39, N. 10, 5 May 2006. https://doi.org/10.1088/0022-3727/39/10/045

[23] -J. Pan, S. Hu, .L. Yang, S. Chen, “Numerical analysis of the heat transfer and material flow during keyhole plasma arc welding using a fully coupled tungsteneplasmaeanode model”, Acta Materialia 118, p. 221-229, 15 July 2016

[24] G. Abdelal and A. Murphy, “A Multiphysics Simulation Approach for Efficient Modeling of Lightning Strike Tests on Aircraft Structures”, IEEE TRANSACTIONS ON PLASMA SCIENCE, VOL. 45, NO. 4, APRIL 2017.